Ionisation and fragmentation dynamics of laser desorbed polycyclic aromatic hydrocarbons using femtosecond and nanosecond post-ionisation

L. Robson[a], A.D. Tasker[a], K.W.D. Ledingham[a,b,*], P. McKenna[a], T. McCanny[a],
C. Kosmidis[c], P. Tzallas[c], D.A. Jaroszynski[d], D.R. Jones[d]

[a] *Department of Physics and Astronomy, University of Glasgow, Glasgow G12 8QQ, Scotland, UK*
[b] *AWE plc, Aldermaston, Reading, Berkshire RG7 4PR, UK*
[c] *Department of Physics, University of Ioannina, GR-45110 Ioannina, Greece*
[d] *TOPS Laser Facility, Department of Physics and Applied Physics, University of Strathclyde, Strathclyde G4 0NG, Scotland, UK*

Abstract

Nanosecond laser desorption/femtosecond laser mass spectrometry (LD/FLMS) incorporating a reflectron time-of-flight mass spectrometer has been used to study the ionisation/fragmentation of polycyclic aromatic hydrocarbons (PAHs) in intense laser fields (7.0×10^{14} to 9.3×10^{15} W cm^{-2}). Pulses of 80 fs, 800 nm have been used to post-ionise the PAHs anthracene, tetracene and pentacene. For each molecule strong singly and doubly charged parent ions are observed accompanied by fragmentation. In addition, strong triply charged parent ions (M^{3+}) are observed for anthracene and weaker M^{3+} signals for tetracene and pentacene are also observed. Nanosecond post-ionisation (266 nm, 16 ns) spectra of the molecules have been recorded and are included for comparison with the femtosecond data. Similarities in the observed fragmentation pattern of low-mass fragments of the nanosecond and low intensity femtosecond spectra are highlighted. In addition, as the laser intensity increases, it is observed that fragmentation pathways preferentially switch from $C_m H_3^+$ ion yield to C_m^+ production for $m = 2$–5 at a critical intensity which is molecule dependent. (Int J Mass Spectrom 220 (2002) 69–85)
© 2002 Elsevier Science B.V. All rights reserved.

Keywords: Laser desorption/femtosecond laser mass spectrometry; Polycyclic aromatic hydrocarbons (PAHs); Multiply charged ions; Field ionisation

1. Introduction

The rapidly developing field of ultrafast laser–molecule interactions has highlighted new areas of physics and chemistry and is becoming an important tool for atomic and molecular analysis [1–5]. From a mass spectrometry perspective, the generation of molecu-

lar or structurally-characteristic ions is a key feature in the technique's analytical ability. The advantages of ultrafast ionisation of atoms and molecules in the gas phase have been identified through comparative studies [6,7] using nanosecond, picosecond and femtosecond laser pulses. The Glasgow/Ioannina group has carried out extensive investigations [8–11] of gas-phase non-resonant femtosecond laser ionisation using time-of-flight (ToF) mass spectrometry.

* Corresponding author. E-mail: k.ledingham@physics.gla.ac.uk

However, the development of FLMS as a general analytical technique requires methods to convert solid phase species to the gas phase for ionisation.

Laser desorption/femtosecond laser mass spectrometry (LD/FLMS) allows ultra-sensitive detection and trace analysis of atoms and molecules from solid phase. The technique involves two steps: desorption of intact neutral molecules from a solid sample surface and post-ionisation of the desorbed analyte using high intensity (10^{14}–10^{15} W cm^{-2}) femtosecond laser pulses. After extraction, the ions are mass-separated and detected according to their mass-to-charge ratio using a reflectron ToF mass spectrometer. The intense, ultrafast pulses from the femtosecond laser are able to ionise virtually any class of molecule reducing considerably the chance of dissociation prior to detection. Amongst other advantages, the temporal and spatial decoupling of desorption and ionisation allows each step to be optimised independently yielding improvements in system performance. In addition, the use of a reflectron ToF mass spectrometer instead of a linear system provides sufficiently high mass resolution ($\sim$1000) in resultant spectra which permits identification of non-integer ion peaks.

In the present study, the technique is applied to the polycyclic aromatic hydrocarbons (PAHs) anthracene (178 Da), tetracene (228 Da) and pentacene (278 Da) which, with the exception of anthracene, cannot be analysed in the gaseous phase. These molecules are fused aromatic rings and are environmental pollutants, formed during the incomplete combustion of organic material. In contrast to similar studies carried out by Markevitch et al. [12] the spectra presented here for the PAHs upon interaction with 80 fs, 800 nm intense femtosecond laser pulses exhibit strong parent ion peaks, accompanied by suppressed fragmentation. Doubly and triply charged parent ions are observed in the present study and each molecule also exhibits a number of doubly charged hydrocarbon groups $C_mH_n{}^{2+}$. Comparative studies adopting nanosecond ionisation have also been carried out for the above mentioned PAHs. The aim of the present paper is to investigate the ionisation and fragmentation of the PAHs using both nanosecond and femtosecond post-ionisation with a high resolution ToF mass spectrometer.

2. Experimental

A schematic of the reflectron ToF mass spectrometer used in the present study is shown in Fig. 1 and has been described in detail previously [13,14]. Briefly, the system comprises of a source chamber and flight tube, pumped using rotary-backed turbomolecular pumps to a base pressure of 10^{-9} Torr, and a rotary pumped sample load-lock. The interaction chamber is spherical, 30 cm in diameter and several ports fitted with fused quartz windows facilitate laser irradiation and direct sample viewing. A two-stage reflectron and MCP detector are contained in the 1.5 m flight tube. Powder samples for analysis are dissolved in a suitable volatile solvent, deposited onto a stainless steel stub, and allowed to dry. A transfer arm is then used to admit the stub into the chamber via the rotary pumped sample load lock. The stub is placed on a manipulator arm in the centre of the chamber to allow movement in three dimensions and rotation about the vertical axis. An ion optic arrangement has been designed especially for this instrument [15] to facilitate ion extraction and acceleration in electric fields. Potentials of +3.0 and +2.5 kV with respect to the field-free flight tube are applied to the sample stage and ion optic, respectively. The ions are accelerated into a reflectron electrostatic mirror before being detected by a multi-channel plate detector (Galileo). A digital oscilloscope (LeCroy 9344C) is used for single-shot and averaged data collection and is connected to a PC installed with GRAMS/32 software (Galactic) through a GPIB interface plug. In this manner, ToF spectra are readily obtained and mass calibration as well as analysis performed.

Laser desorption of the solid samples was achieved using the fourth harmonic output (266 nm, 5 ns) from a Nd:YAG laser (Minilite I, Continuum) focused onto the sample stub. The energy of the desorption laser beam was controlled using an optical attenuator (Newport, 935-5) and monitored using a joulemeter.
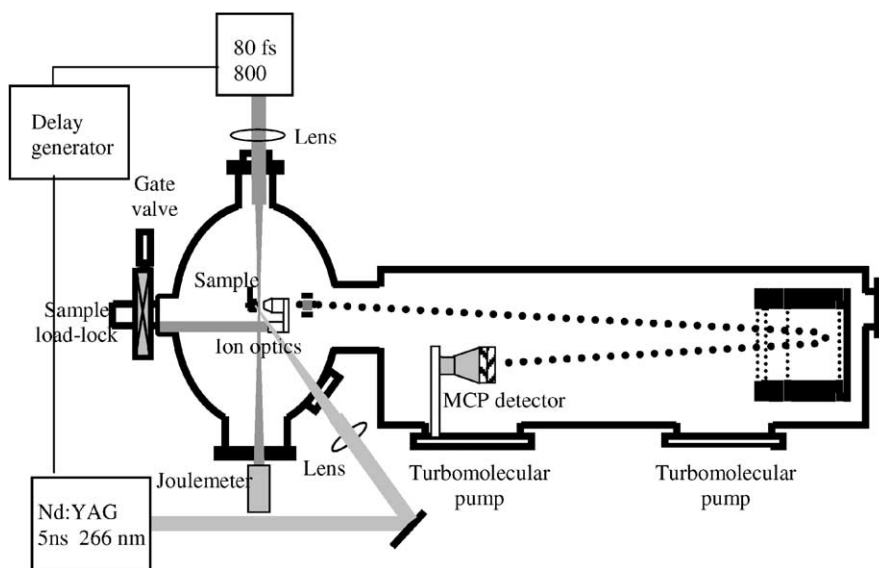
Fig. 1. Schematic of the experimental set-up.

A 27 cm focal length lens was used to focus the beam (~7 mm) yielding intensities of up to $1 \times 10^{10}\,\mathrm{W\,cm^{-2}}$ for desorption.

Femtosecond post-ionisation was performed using the Strathclyde Terhertz to Optical Pulse Source (TOPS) femtosecond laser system [16]. To produce the seed pulse for the system a Ti:sapphire Femtosource F220 laser was employed, this was pumped with a VERDI CW laser (532 nm, 5 W). The repetition rate of the oscillator was 76 MHz with an average power output of 500 mW, generating pulses of 7 nJ with a pulse length of 20 fs. The low energy, ultrashort pulses are then stretched to 200 ps before being amplified in a 10 Hz, 10 ns, Nd:YAG pumped regenerative Ti:sapphire amplifier. Two further amplifiers generate the pulse of required energy: first a two pass amplifier, pumped by the same YAG as the Regenerative Amplifier, secondly an eight pass amplifier pumped by two 10 Hz, 8 W SAGA YAGs. The amplified pulses are re-compressed using a grating. This set-up delivered laser pulses of 250 mJ, and temporal pulse widths (FWHM) of 80 fs (as measured by an autocorrelator) at 800 nm. A beam splitter provided the required energy and variable attenuation of the beam (0.25–7 mJ) was achieved using absorptive

neutral density filters. Focussing the ~1 cm diameter beam using a 30 cm focal length lens provided intensities as high as $2 \times 10^{16}\,\mathrm{W\,cm^{-2}}$.

Nanosecond post-ionisation of PAHs was achieved using the fourth harmonic output (266 nm) of a second Nd:YAG laser (SL2Q/SL3A, Spectron Laser System). The 16 ns pulse was focussed using a 30 cm focal length lens generating intensities of up to $2.5 \times 10^9\,\mathrm{W\,cm^{-2}}$.

3. Results and discussion

Time-of-flight mass spectra for anthracene, tetracene and pentacene are shown in Figs. 2–4, respectively. For each spectrum, areas of multiply charged molecular ions and singly charged parent ion have been expanded for ease of identification. Each molecule was studied over a range of intensities (7.0×10^{14} to $9.3 \times 10^{15}\,\mathrm{W\,cm^{-2}}$) but the data presented in Figs. 2–4 was recorded at $1.5 \times 10^{15}\,\mathrm{W\,cm^{-2}}$. Typical laser intensities for desorption were 3–$6 \times 10^8\,\mathrm{W\,cm^{-2}}$ with the exception of anthracene which was sublimed directly from the sample stub as the addition of the desorption laser
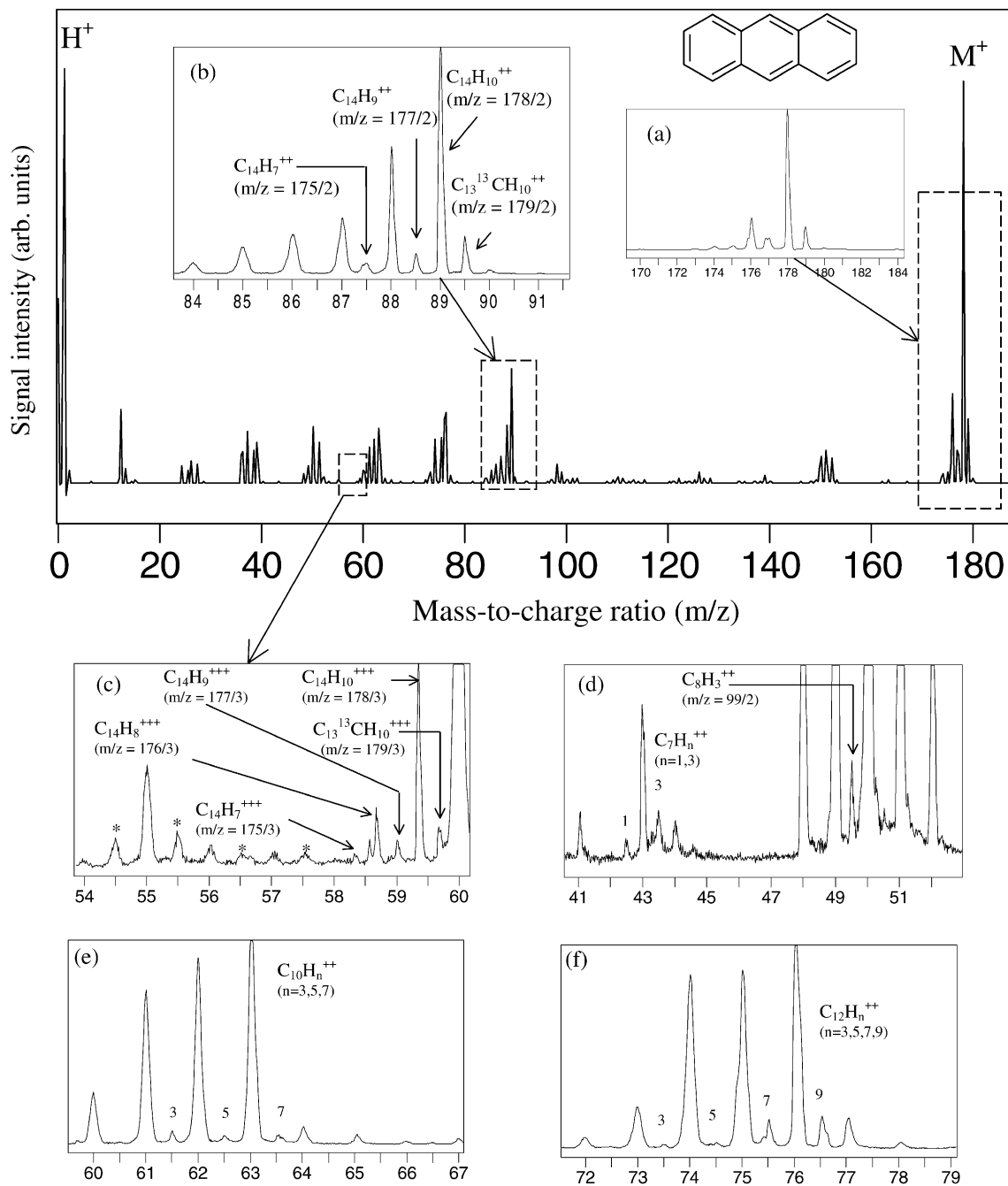
Fig. 2. ToF mass spectra of laser desorbed anthracene ($m/z = 178$) irradiated using 80 fs, 800 nm at an intensity of 1.5×10^{15} W cm^{-2}. Parts (a) and (b) show singly and doubly charged parent ion, respectively. Part (c) shows triply charged parent and surrounding satellite ions, as well as unambiguous $C_m H_n^{2+}$ fragments denoted by asterisk (*). Various doubly charged $C_m H_n^{2+}$ carbon groups are shown in (d)–(f).
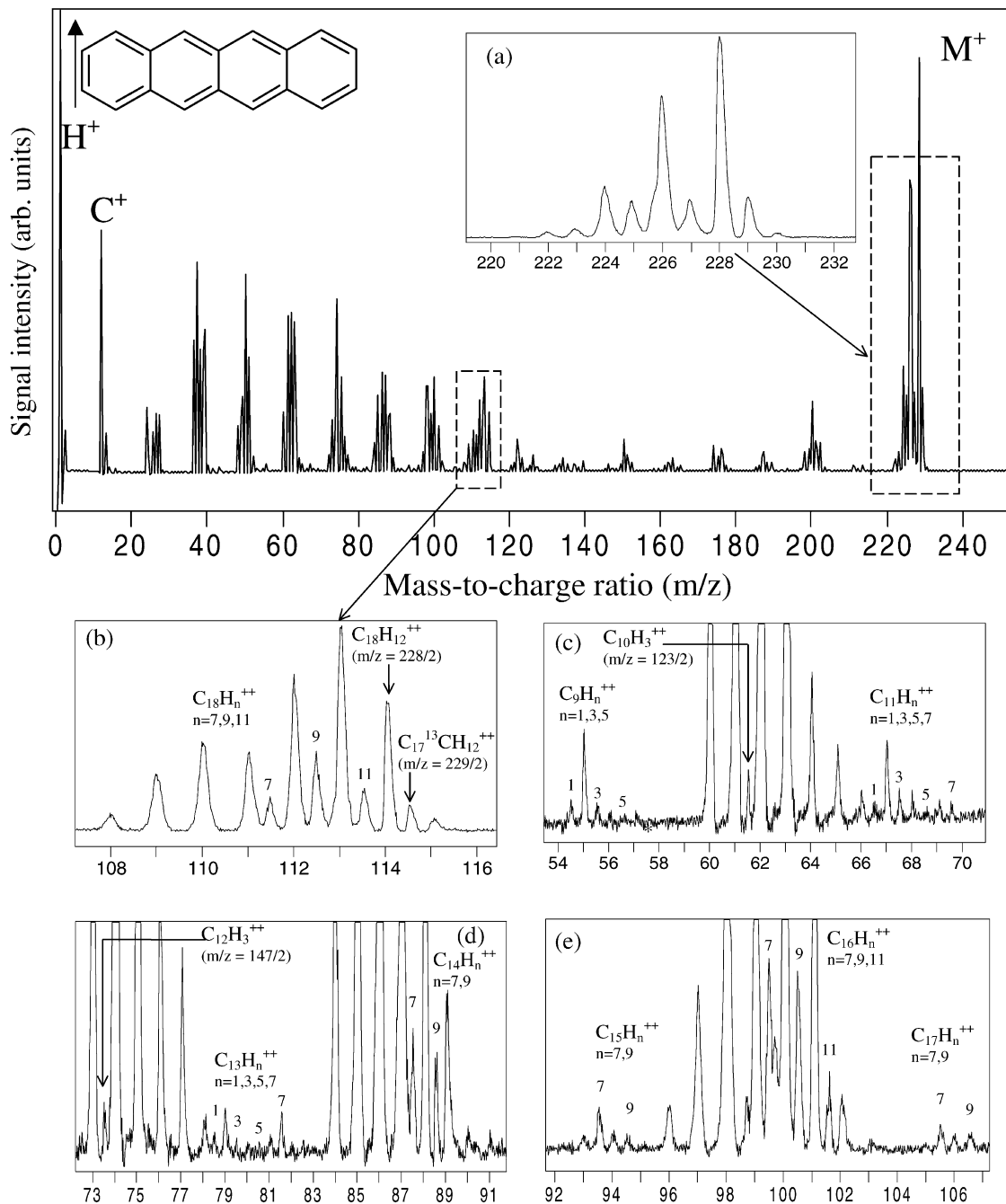
Fig. 3. ToF mass spectra of laser desorbed tetracene ($m/z = 228$) irradiated using 80 fs, 800 nm at an intensity of $1.5 \times 10^{15} \, W \, cm^{-2}$. Parts (a) and (b) show singly and doubly charged parent ion, respectively. Parts (c)–(e) show unambiguous doubly charged carbon groups $C_mH_n^{2+}$.
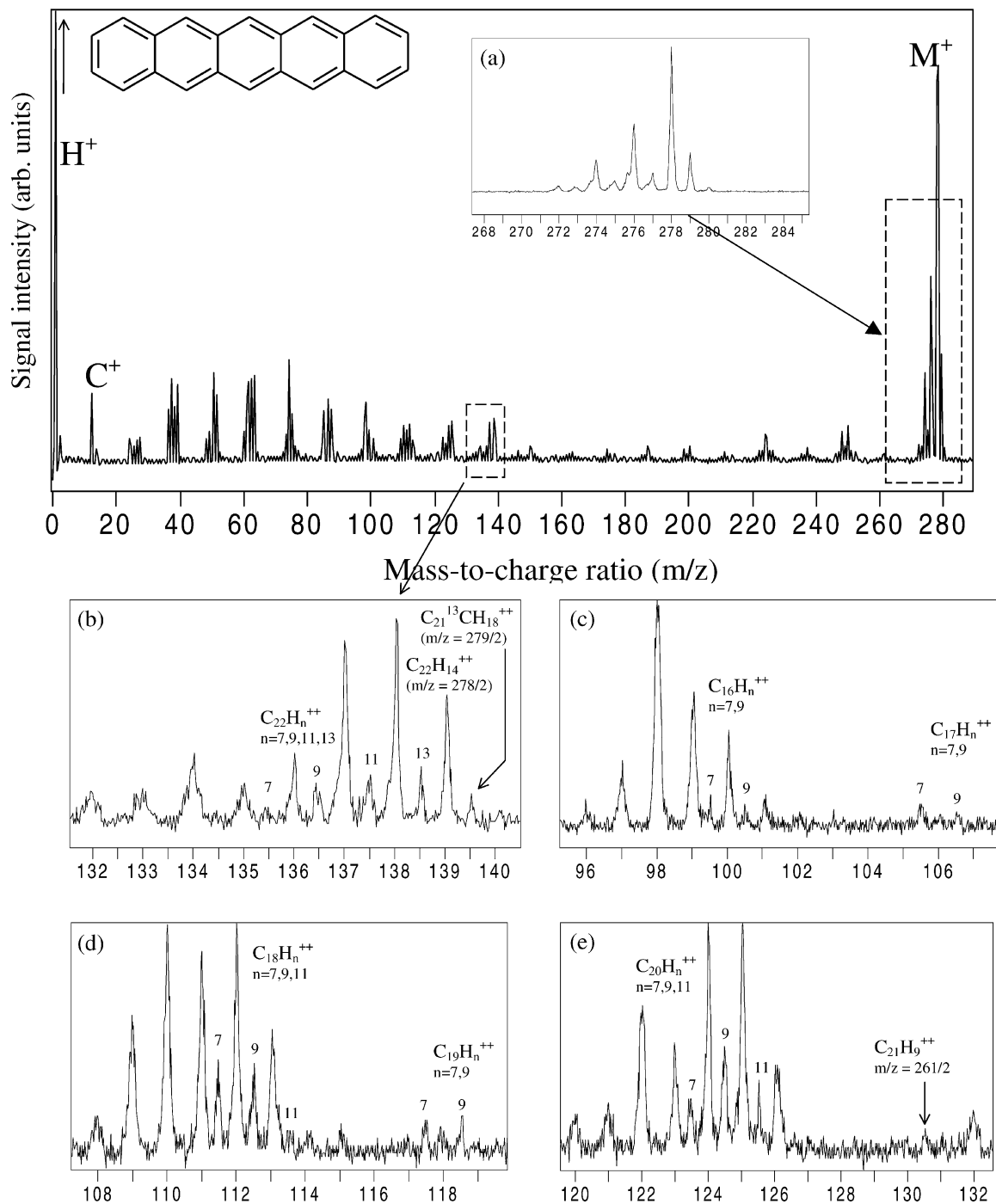
Fig. 4. ToF mass spectra of laser desorbed pentacene ($m/z = 278$) irradiated using 80 fs, 800 nm at an intensity of 1.5×10^{15} W cm^{-2}. Parts (a) and (b) show singly and doubly charged parent ion, respectively. Parts (c)–(e) show unambiguous doubly charged carbon groups $C_m H_n^{2+}$.

made no measurable difference to the total ion signal. A strong H^+ is present in all spectra at the given intensities and in some cases is the base peak. A mass resolution of 1000 was routinely obtained, allowing non-integer m/z values to be easily distinguished.

3.1. Anthracene ($C_{14}H_{10}$)

A strong molecular parent ion is observed at $m/z = 178$ in Fig. 2 and the region around the molecular ion has been expanded. A substantial doubly ionised anthracene parent ion is also observed at $m/z = 89$, shown in Fig. 2(b). Surrounding peaks between $m/z = 87.5$ and 89.5, separated by half mass units, have been identified as $C_{14}H_7^{2+}$ to $C_{13}{}^{13}CH_{10}^{2+}$, although peaks lying at integer m/z values in this envelope will inevitably contain some degree of singly charged component $C_7H_n^+$. In particular, the peak at $m/z = 89$ may also be assigned to $C_7H_5^+$, but this is considered to make only a small contribution ($<1\%$) to the yield of the peak. This is confirmed by considering the isotopic abundances of $^{13}C/^{12}C$. A natural isotopic mixture [17] of 98.9% ^{12}C and 1.1% ^{13}C exists for carbon and so for a molecule containing m carbon atoms, we would expect approximately ($m \times 1.1$)% ^{13}C in resulting spectra. For anthracene ($C_{14}H_{10}$), the isotopic ratio of $C_{13}{}^{13}CH_{10}^+/C_{14}H_{10}^+$ (peaks at $m/z = 178$ and 179) is ~15% and the measured peak areas agree well with this value. The ratio of the peaks at $m/z = 89.5$ and 89 is also 15%, confirming the dominance of $C_{14}H_{10}^{2+}$ at $m/z = 89$. Fig. 2(c) shows triply charged parent ion ($C_{14}H_{10}^{3+}$, $m/z = 178/3$) and adjacent satellite triply charged ions, ($C_{14}H_7^{3+}$ to $C_{13}{}^{13}CH_{10}^{3+}$) all separated by third mass units. Again, the isotope ratio ($C_{13}{}^{13}CH_{10}^{3+}/C_{14}H_{10}^{3+}$) is consistent, ~15%, which is as expected since both peaks are unambiguously identified due to their m/z values. Although the peak at $m/z = 59$ lies at an integer value, it cannot be attributed to any $C_4H_n^+$ combination and is unlikely to be $C_9H_{10}^{2+}$ as no peak is evident at $m/z = 59.5$. Also occurring below this triply charged envelope are peaks at half m/z values indicating the unambiguous presence of doubly charged species. These are C_9H^{2+}, $C_9H_3^{2+}$, $C_9H_5^{2+}$

and $C_9H_7^{2+}$ corresponding to $m/z = 54.5, 55.5, 56.5$ and 57.5, respectively and have been suitably identified by asterisk (*) in the figure. Surrounding peaks at integer m/z values will inevitably be a combination of singly ionised hydrocarbon fragments, ($C_4H_n^+$, $n = 6$–9) and doubly ionised hydrocarbon fragments ($C_9H_n^{2+}$, $n = 0, 2, 4, 6$). Fig. 2(d)–(f) show various doubly ionised hydrocarbon fragments also observed for anthracene. Fig. 2(d), for example, shows such fragments at $m/z = 42.5$, attributed to C_7H^{2+}, also $m/z = 43.5$ ($C_7H_3^{2+}$) and $m/z = 49.5$ ($C_8H_3^{2+}$). Again, unambiguous identification is possible since these peaks lie at half integer values. The remaining unambiguous doubly ionised molecular fragments are highlighted in Fig. 2(e) and (f).

3.2. Tetracene ($C_{18}H_{12}$)

A strong parent ion is observed at $m/z = 228$ in Fig. 3. Again, the doubly ionised parent ion ($C_{18}H_{12}^{2+}$) is observed at $m/z = 114$ and confirmed by the presence of $C_{17}{}^{13}CH_{12}^{2+}$ at $m/z = 114.5$ with a consistent isotopic ratio of ~19% as expected for tetracene. An envelope of doubly charged components is also evident around the $C_{18}H_{12}^{2+}$ ion ($m/z = 111.5$–114.5). Furthermore, a number of doubly ionised hydrocarbon fragments are observed, shown in the remaining insets. Fig. 3(c) shows distinguished doubly ionised fragments assigned to ($C_9H_n^{2+}$, $n = 1, 3, 5$), $C_{10}H_3^{2+}$, and ($C_{11}H_n^{2+}$, $n = 1, 3, 5, 7$), at half m/z values. Peaks positioned at integer m/z values that are surrounded by unambiguous doubly ionised fragments at half m/z values are thought to contain some degree of doubly ionised component. Highlighted in Fig. 3(d) and (e) are various $C_mH_n^{2+}$ fragments, again all unambiguous doubly ionised entities have been identified. It should be noted that for tetracene at intensities $>4 \times 10^{15}\,W\,cm^{-2}$ (not shown), a small peak is evident at $m/z = 229/3$ attributed to $C_{17}{}^{13}CH_{12}^{3+}$ confirming the presence of a triply charged parent ion at $m/z = 228/3$. The single and double ionisation of PAHs of varying size and structure has also been addressed recently by Schröder et al. [18].

3.3. Pentacene ($C_{22}H_{14}$)

This spectrum exhibits a strong parent ion peak at $m/z = 278$, expanded in Fig. 4(a). A prominent doubly ionised parent ion is evident at $m/z = 139$, surrounded by an envelope of doubly charged components, as shown in Fig. 4(b). Furthermore, a consistent isotopic ratio of approximately 23% exists which is slightly lower than expected but within experimental accuracy and can possibly be explained by the presence of $C_{11}H_7^+$ at $m/z = 139$. Various doubly charged hydrocarbons are observed and are indicated in Fig. 4(c)–(e). As with anthracene and tetracene, it is only those fragments which lie at half m/z values that can be uniquely assigned to doubly ionised entities, although it is reasonable to assume that the surrounding peaks coinciding with integer m/z values contain some degree of doubly charged entities. In addition it should be pointed out that for pentacene, peaks were observed attributed to triply charged parent ions, $C_{22}H_{14}^{3+}$ and adjacent triply charged satellite ions at intensities $>2.5 \times 10^{15}\,\text{W cm}^{-2}$.

The data presented here for anthracene tetracene and pentacene are broadly similar, with strong parent ion signatures accompanied by suppressed fragmentation observed and is in contrast to the findings of Markevitch et al. [12] who reported diminished parent ion and a high yield of fragmentation for anthracene and tetracene. It is difficult to account for these discrepancies because in both studies the femtosecond lasers are similar in wavelength and pulse duration but several possibilities exist such as non-linear effects in the laser beam, for example self focusing. This is a deleterious effect when a high intensity laser beam propagates through a medium, e.g., optics and chamber windows where the index of refraction changes non-linearly with the intensity and can be described by the B-integral [19–21]. Significant distortion occurs when B is of the order of 5. The B-integral is given by

$$B = \frac{2\pi n_2}{\lambda} \int_0^z I(t, z)\, \mathrm{d}z$$

where n_2 is the non-linear refractive index of a material [19], λ the wavelength and $I(t, z)$ is the intensity

of the laser pulse in the medium under consideration. In the present study the accumulative B for air and optics is measured as ∼3 although most authors do not quote the B value. Significant distortion of the beam can occur when $B > 5$. Assion et al. [22] have shown that the relative yield of fragmentation in mass spectra is significantly altered when the laser pulse is distorted. A cross-correlation of the pulse at 800 nm is shown in Fig. 5. It can be seen that a small pre-pulse is present at ∼6 ps before the femtosecond pulse. This may lead to intensities high enough to form pre-plasmas in the interaction region but is not thought to contribute significantly to the present data. If, however, any pre-pulses were of a higher relative intensity compared with the main pulse then a significant contribution could be expected.

For each of the PAHs studied the profile of the molecular ion in the resultant mass spectra exhibits a similar trend. Predominant peaks around the parent envelope correspond to an even number of hydrogen atoms removed from the parent ion (see Figs. 2–4). Tzallas et al. [23] observed the loss of 2, 4 and 6 hydrogen atoms from the non-aromatic molecular ion thiazolidine and concluded that the loss of an even number of hydrogen atoms is more probable than the loss of odd numbers from the parent ion. This observation implies the enhanced stability of these structures where hydrogen pairs have been removed. For the aromatics studied here, the same preferential stripping of an even number of hydrogens is observed. It should be noted that this feature has previously been observed for aromatics [24], but the process is generally more pronounced in the doubly charged parent ion as discussed for toluene in reference [11]. Furthermore, for each of the PAHs in the present study it is postulated that the same preferential loss of even pairs (n) of hydrogen atoms is occurring in the doubly charged parent ions $[M - nH_2]^{2+}$ as shown in Figs. 2(b), 3(b) and 4(b), but since the doubly charged parent envelope coincides with singly charged $C_mH_n^+$ species then this determination is somewhat ambiguous.

It is also apparent on inspection of each of the spectra (Figs. 2–4) that a general pattern can be observed for the ion yield of the high mass $C_mH_n^+$ fragments.
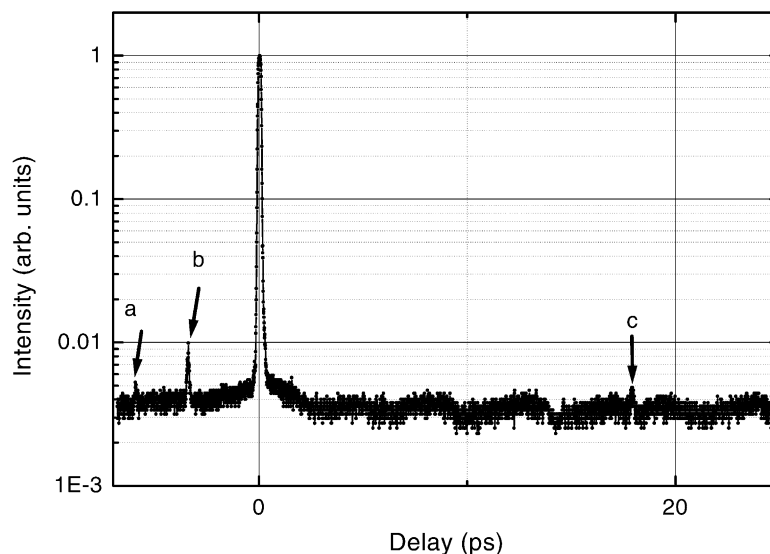
Fig. 5. Cross-correlation of pulse showing (a) pre-pulse at -5.97 ps, (b) a reflection from the SHG crystal at -3.39 ps and (c) a post-pulse at $+17.9$ ps.

For the three molecules, anthracene, tetracene and pentacene, $C_m H_n^+$ groups exist from C_1 to $C_{14, 18, 22}$, respectively (n arbitrary). For $C_m H_n^+$ groups with $m \geq 12$, those with even numbers of carbons have a greater yield than those with odd numbers producing an 'odd–even' carbon effect. In the case of pentacene, the largest of the three molecules, this effect is most pronounced and for odd values of m, $C_m H_n^+$ fragments are negligible. For $m \leq 12$ this effect is not observed to any great degree. The C_2 fragment is preferentially lost as the $C_m H_n^+$ fragment size increases and a similar feature was observed by O'Brien et al. [25] for carbon clusters greater than C_{34}.

Many studies have been carried out to investigate the ionisation of medium mass molecules in intense laser fields [8,26–28]. The Glasgow/Ioannina collaboration first reported doubly and triply ionised molecular ions for medium mass aromatic molecules benzene, monodeuterated benzene and naphthalene [24]. Since then, various studies [4,29–31] have been carried out to investigate the ionisation mechanism and pathways of aromatic molecules for singly and multiply charged ion production. Molecular ionisation could be attributed to multiphoton ionisation and/or a

field ionisation mechanism, although at the intensities at which the present data has been recorded ($I > 10^{15}$ W cm^{-2}), it is generally accepted that field ionisation is the dominant mechanism [32]. The Keldysh parameter γ, which is used to determine the degree of multiphoton and field ionisation mechanisms [33,34], places the present ($\gamma \sim 0.2$) results well within the field ionisation regime. Also associated with short pulse high intensity lasers is a phenomenon known as coulomb explosion [29,35]. At high intensities multiply charged transient molecular species are formed which are subject to considerable coulomb repulsion. This can result in an explosion of the molecule producing stable ions with high kinetic energies. The appearance of stable multiply charged atomic ions in the mass spectra is evidence of coulomb explosion. Fragments can be ejected in the forward and backward (with respect to the ToF axis) directions resulting in a split peak structure. A small peak at $m/z = 6$ (C^{2+}) is observed for the three molecules studied at this intensity (1.5×10^{15} W cm^{-2}), commensurate with the onset of coulomb explosion. As the intensity was increased, C^{2+} yield increased and C^{3+} was observed for each of the molecules. Concern-
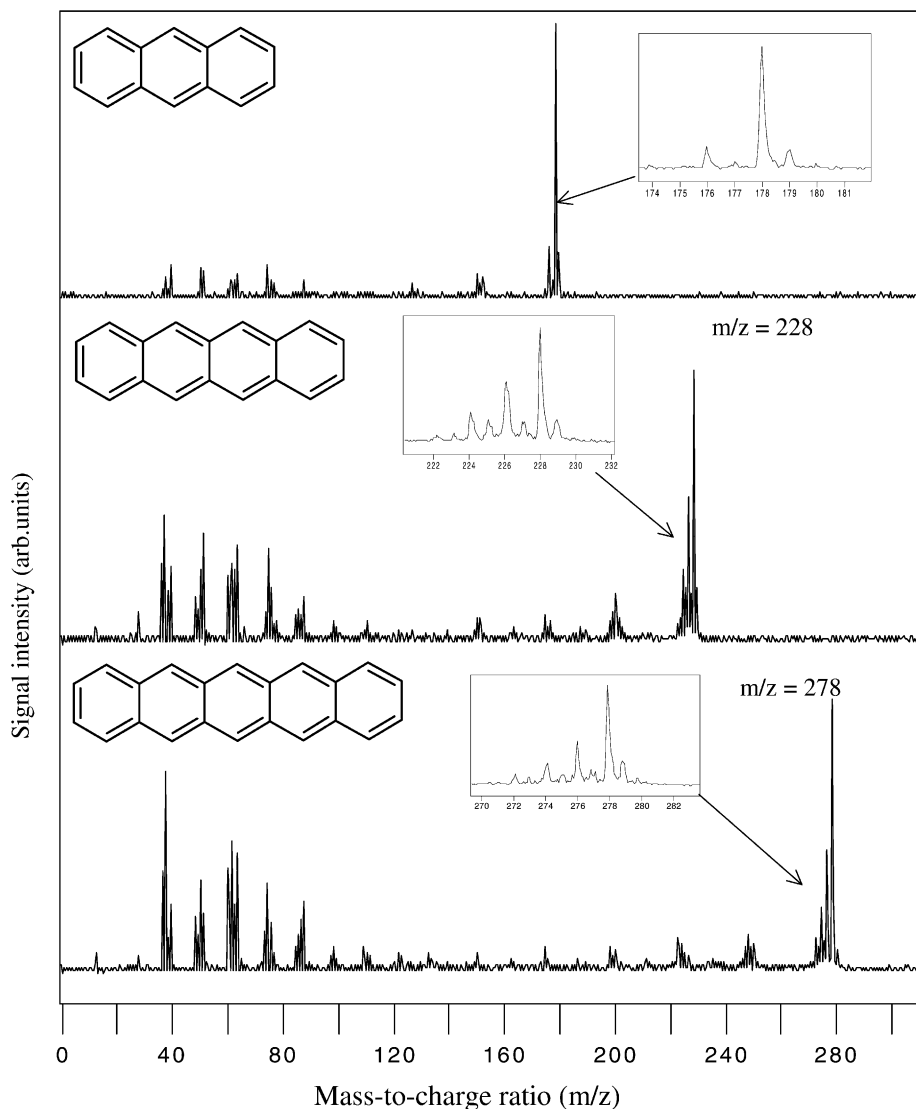
Fig. 6. ToF mass spectra of laser desorbed anthracene, tetracene and pentacene irradiated using 16 ns, 266 nm at an intensity of $1.2 \times 10^9 \, \text{W cm}^{-2}$. Each molecule displays prominent parent molecular ion.

ing the pathways for single and multiple charged ion production Cornaggia [36] suggested that the single ionisation of molecules under intense laser irradiation occurs at the beginning of the laser pulse, for a typical Guassian profile, and then multiple ionisation appears for higher instantaneous laser intensities along the pulse profile. However, recent studies [26] of small molecules, N_2, C_2H_2 and C_3H_4 have provided

Fig. 7. ToF mass spectra of tetracene as a function of relative intensity for nanosecond (a)–(c) and femtosecond (d)–(f) pulses. For the lowest intensities at both pulse lengths, (a) and (d), the fragmentation pattern exhibited by the C_3 to C_6 groups are similar, indicating a common pathway between the mechanism of fragmentation. The insets show C_3^+ to $C_3H_3^+$ for each pulse length.

Relative signal Intensity

C$_3$

266 nm, 16 ns,
I = 1.2 x 10^9 Wcm^{-2} (a)

C$_3$

266 nm, 16 ns,
I =1.7 x 10^9 Wcm^{-2} (b)

266 nm, 16 ns,
I = 2.2 x 10^9 Wcm^{-2} (c)

800 nm, 80 fs,
I = 1.5 x 10^{15} Wcm^{-2} (d)

C$_3$

C$_3$

800 nm, 80 fs,
I = 4.4 x 10^{15} Wcm^{-2} (e)

800 nm, 80 fs,
I = 9.3 x 10^{15} Wcm^{-2} (f)

Mass-to-charge ratio (m/z)
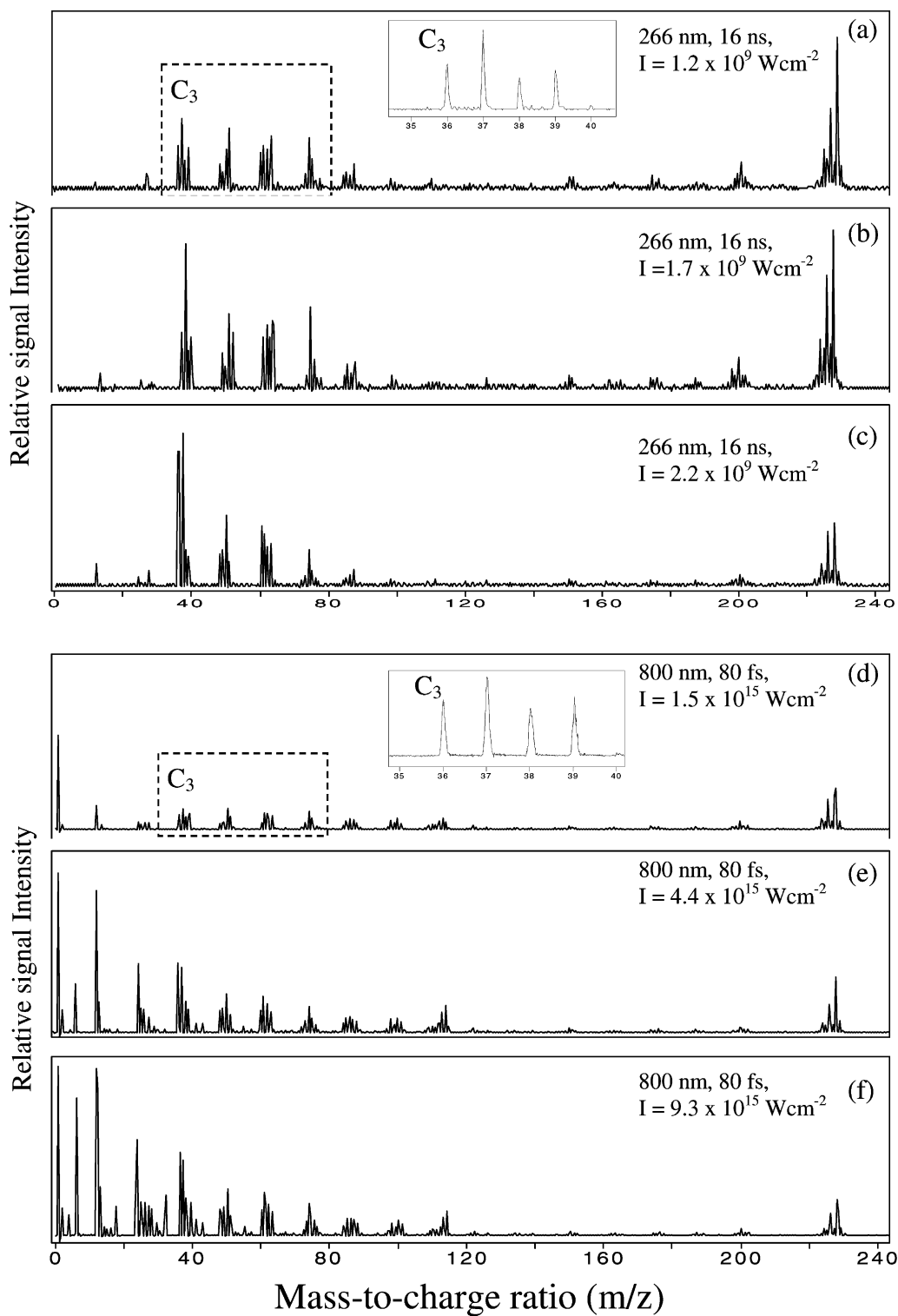
evidence that non-sequential electron emission plays an important role in high intensity laser fields. The single and multiple ionisation of molecules remains an active area of research.

Comparative studies were carried out to characterise laser-desorbed PAHs under nanosecond ionisation conditions. Fig. 6 shows mass spectra of laser desorbed anthracene, tetracene and pentacene post-ionised using 266 nm, 16 ns laser pulses at an intensity of 1.2×10^9 W cm^{-2}. From the insets shown it can be seen that the parent ion exhibits the same preferential stripping of pairs of hydrogen atoms as in the femtosecond mass spectra. Also, $C_mH_n^+$ fragments are more prominent for even m, where $m \geq 12$ as was observed in the case of femtosecond irradiation. For each molecule, parent ion peaks are the main components of the spectra with minimal fragmentation observed. DeWitt and Levis have studied the relationship between molecular structure and the associated ionisation/dissociation of PAHs under strong laser fields and observed an exponential increase in molecular dissociation as the number of atoms in a series increases [2,30]. The data presented here for both nanosecond and femtosecond ionisation seems to agree with these findings as far as anthracene and tetracene are concerned but apparently pentacene does not follow the same trend. As expected, no multiply charged molecular ions were observed under nanosecond irradiation at the associated ionisation intensities. The fragmentation pattern of low mass carbon groups (C_3H_n to C_6H_n) exhibited by the PAHs under nanosecond post-ionisation (UV irradiation) is similar to that of femtosecond (IR) conditions as shown in Figs. 2–4 at the given intensities. To highlight this further, Fig. 7 shows ToF mass spectra of laser desorbed tetracene over a range of intensities using both nanosecond (a)–(c) (1.2–2.2 × 10^9 W cm^{-2}) and femtosecond (d)–(f) (1.5–9.3 × 10^{15} W cm^{-2}) laser pulses. The fragmentation pattern at each intensity is determined

by the appearance of the carbon groups and their intensity yield compared to the molecular ion. For the nanosecond data, parent ion dominates the spectra at lower intensities but as the intensity increases low mass fragmentation yield increases (in particular the C_3 group) and diminished parent ion is observed. A similar pattern has been observed previously by Dietz et al. for benzene [37] under UV ionisation. This can be attributed to dissociation from ionic state manifold. In the case of the femtosecond-induced spectra, as the intensity increases (Fig. 7(e) and (f)), multiply charged carbon atoms have been observed. This is indicative of coulomb explosion. For the lowest laser intensity used at each pulse length, the overall fragmentation pattern exhibited by the low mass carbon groups ($C_3H_n^+$ to $C_6H_n^+$) is similar, as well as the individual carbon group profiles, as shown in the insets. It is well known that nanosecond UV irradiation of aromatics in the intensity regime 10^9 W cm^{-2} and above yields extensive fragmentation with dissociation of these molecules taking place in the single ion manifold [38]. Since femtosecond irradiation produces similar mass spectra it is felt that the same dissociative states are reached although necessarily by different pathways. The mechanism of fragmentation of molecules in intense laser fields is an important but complex problem and has been addressed in recent papers [29,39].

In addition, one important difference between the spectra at each pulse length exists. For the nanosecond data, once the onset of fragmentation is established (~2.5 × 10^8 W cm^{-2} for tetracene), the individual $C_mH_n^+$ distribution pattern remains unaltered as the intensity increases. For the femtosecond spectra this is not the case. Fig. 8 shows the laser intensity dependence for low mass fragments C_m^+ and $C_mH_3^+$ ($m = 2$–6) and C^{2+} for tetracene between 7.0 × 10^{14} and 9.4 × 10^{15} W cm^{-2}. In Fig. 8(a) it is observed that for the C_2 group at the lowest intensity the ion yield

▶

Fig. 8. Dependence of ion yield vs. laser intensity for tetracene for low mass fragments (a) C_2^+ and $C_2H_3^+$, (b) C_3^+ and $C_3H_3^+$, (c) C_4^+ and $C_4H_3^+$, (d) C_5^+ and $C_5H_3^+$ and (e) C_6^+ and $C_6H_3^+$. The laser intensity dependence of C^{2+} is also plotted on each graph. For (a)–(d) it is shown that the fragmentation pathway preferentially switches from $C_mH_3^+$ ion yield to the naked C_m^+ fragment at critical intensities but this trend is not observed for the C_6^+ and $C_6H_3^+$ fragments.
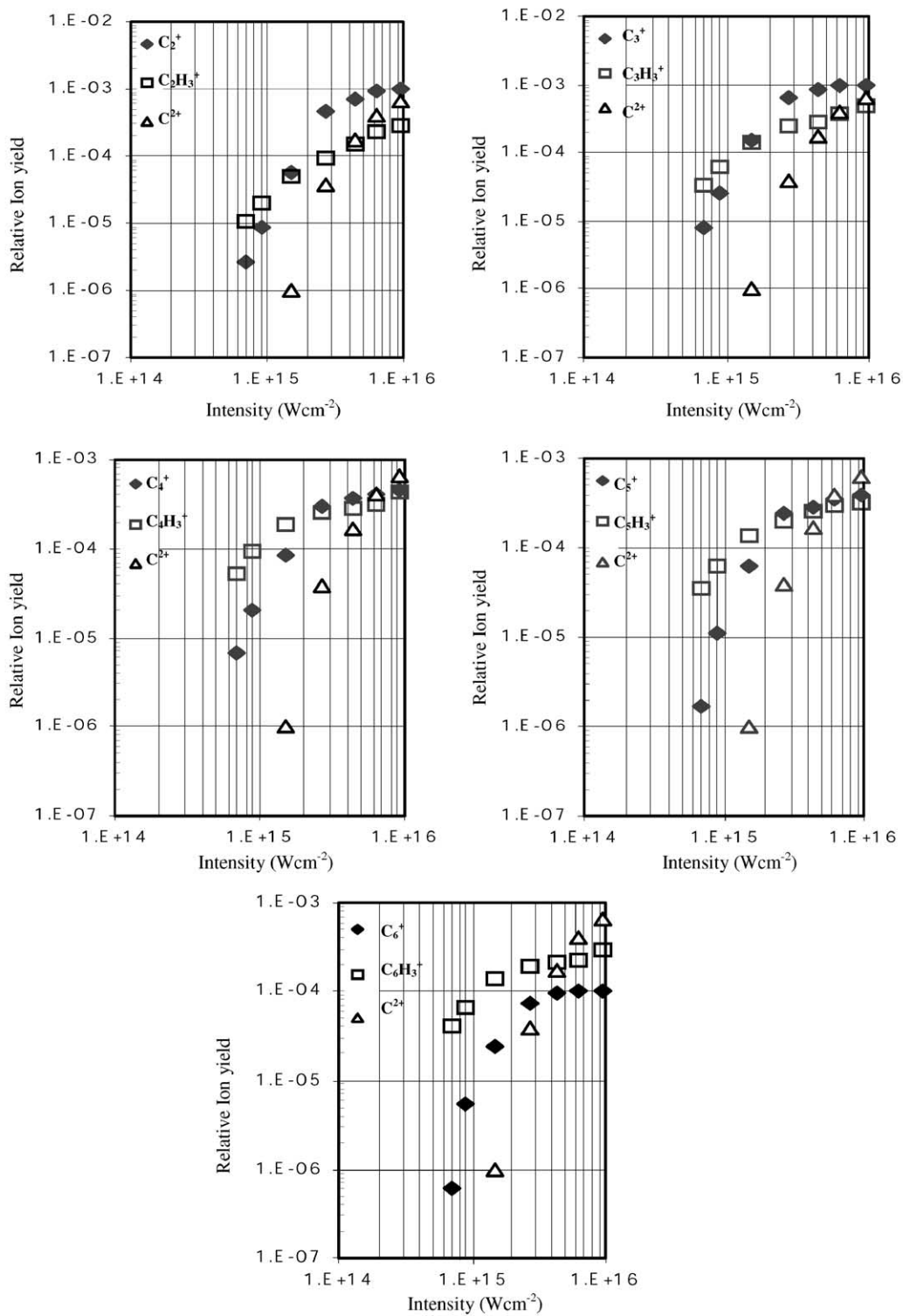
of $C_2H_3^+$ is almost half an order of magnitude greater than the naked C_2^+ fragment. But the C_2^+ peak exhibits a greater intensity dependence and at an intensity of approximately $1.5 \times 10^{15}\,\mathrm{W\,cm^{-2}}$ becomes the dominant peak. At the highest intensity employed ($9.4 \times 10^{15}\,\mathrm{W\,cm^{-2}}$) the C_2^+ ion yield is almost four times that of $C_2H_3^+$. From the same figure a small yield of C^{2+} is observed at an intensity of $\sim 1.5 \times 10^{15}\,\mathrm{W\,cm^{-2}}$ and is commensurate with coulomb explosions. It is at the same approximate intensity an interception point occurs between the C_2^+ and $C_2H_3^+$ ion yield. The same trend is observed for C_3^+ and $C_3H_3^+$ fragments with the ratio of $C_3^+/C_3H_3^+$ yield at the highest laser intensity equal to 3. For both the C_4 and C_5 groups, at an intensity of $\sim 2.5 \times 10^{15}\,\mathrm{W\,cm^{-2}}$, the bare C_m^+ ion yield succeeds that of the fragment $C_mH_3^+$ and the ratio of $C_4^+/C_4H_3^+$ and $C_5^+/C_5H_3^+$ measure 1.2 and 1.1, respectively, at the highest laser intensity. However, for the C_6 group there is no intensity at which the C_6^+ fragment yield surpasses that of $C_6H_3^+$. It can be seen that at critical intensities, fragmentation pathways preferentially switch from $C_mH_3^+$ ion yield to naked C_m^+ fragments in the case of $m = 2$–5. This critical intensity is fragment dependent as can be seen in Fig. 8, however, for each carbon group (C_2 to C_5) this value lies close to the threshold intensity of C^{2+} production which provides direct evidence of a coulomb explosion mechanism. It is likely therefore that some contribution to the C_m^+ ion yield could arise from events involving coulomb explosions of highly charged transient species.

The same pattern exists for low mass fragments C_m^+ and $C_mH_3^+$ in anthracene and pentacene ($m = 2$–5) although the critical intensity at which the C_m^+ ion yield surpasses the $C_mH_3^+$ ion yield decreases with increasing molecular size. For the C_2^+ and C_3^+ ion fragments, the critical intensity is approximately $2.4 \times 10^{15}\,\mathrm{W\,cm^{-2}}$ for anthracene, $1.5 \times 10^{15}\,\mathrm{W\,cm^{-2}}$ for tetracene and $1.4 \times 10^{15}\,\mathrm{W\,cm^{-2}}$ for pentacene. The C_4^+ and C_5^+ fragment yield succeeds the corresponding $C_mH_3^+$ ion signal at $9.0 \times 10^{15}\,\mathrm{W\,cm^{-2}}$ for anthracene, $2.7 \times 10^{15}\,\mathrm{W\,cm^{-2}}$ for tetracene and $2.5 \times 10^{15}\,\mathrm{W\,cm^{-2}}$ for pentacene.
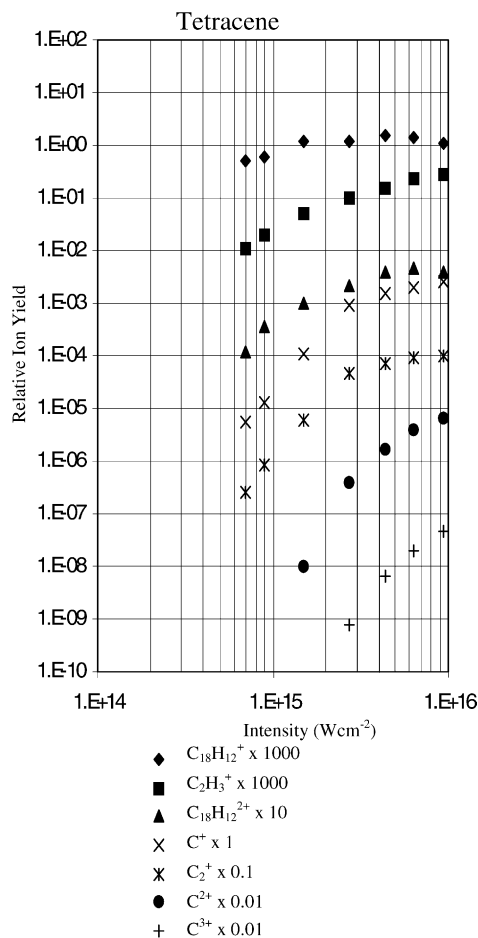
Fig. 9. Dependence of ion yield vs. laser intensity for tetracene for $C_{18}H_{22}^+$, $C_2H_3^+$, $C_{18}H_{22}^{2+}$, C^+, C_2^+, C^{2+}, and C^{3+} fragments. The ion plots are separated by multiplication factors for ease of viewing. The gradient of the doubly charged parent peak follows a steeper slope to the singly charged parent ions. Of the remaining fragments, the $C_2H_3^+$ ion yield follows a more moderate slope than the naked C_m^+ ($m = 1$, 2) or the C^{2+} and C^{3+} peaks.

Fig. 9 shows the ion yield as a function of intensity for several fragment peaks, including singly and doubly charged parent ions for tetracene. Vertical multiplication factors are indicated to separate the ion plots for ease of viewing. It is observed that the dependence of ion yield as a function of laser intensity is not the same for individual peaks. The doubly charged parent ion (M^{2+}) has a greater laser intensity dependence than the singly charged (M^+). The remaining

ion plots include the C_2^+ and $C_2H_3^+$ fragments discussed earlier. It can be seen that the C_2^+ dependence on laser intensity follows a similar gradient to that of the doubly charged parent ions and the C^{2+} and C^{3+} fragments. The same observation is made for the C^+ ion laser intensity dependence. However, the $C_2H_3^+$ ion yield exhibits a more moderate laser intensity dependence similar to that of the parent ion suggesting production of the $C_2H_3^+$ occurs within the parent ion. This trend was observed for all three molecules studied. A similar feature has been observed for benzaldehyde where several mass peaks followed the same laser intensity dependence gradient as the parent ion (apart from the doubly charged parent ion, C^+ and H^+) suggesting a common parent precursor in an ionisation followed by dissociation model [40].

4. Conclusions

Laser-desorption has been coupled to femtosecond laser ionisation mass spectrometry (LD/FLMS) to study the ionisation and fragmentation of solid phase PAHs. The PAHs anthracene (178 Da), tetracene (228 Da) and pentacene (278 Da) have been studied under both femtosecond (800 nm) and nanosecond (266 nm) post-ionisation. Analysis of the mass spectra has demonstrated that strong parent ions accompanied by suppressed fragmentation can be observed for each molecule under both femtosecond and nanosecond regimes.

Doubly charged parent ions were observed for each molecule under femtosecond irradiation surrounded by an envelope of doubly charged satellite peaks $[M - nH_2]^{2+}$. For anthracene, strong triply charged parent ion was also visible, again surrounded by a number of peaks separated by third mass units assigned to $[M - nH_2]^{3+}$. For tetracene and pentacene, small peaks were evident for triply charged parent ion. It has been reported that pre- or post-pulse irradiation (intensity $\sim$ 1/3 of the main pulse) prevents production or survival of trications for small molecules [41]. In the present study pre- and post-pulses have been measured, but are weak enough ($\sim$1%) so

that production and survival of trications is not prevented.

A substantial number of peaks appearing at half m/z integer values were also evident for each molecule and have been attributed to doubly charged high mass $C_mH_n^{2+}$ species. From studies carried out on smaller molecules [26], evidence exists that suggests non-sequential electron emission plays an important role in the double ionisation of molecules in high intensity laser fields, although it is an active area of current research.

It has been well documented that ion fragmentation patterns depend on the pulse length [6,7,40,42] used to irradiate the neutral molecule but some similar features do exist between the fragmentation pattern exhibited by femtosecond and nanosecond irradiation of PAHs in the present study. At intensities of $>10^9$ W cm^{-2} for nanosecond pulses and $<1.5\times10^{15}$ W cm^{-2} for femtosecond pulses, the fragmentation pattern exhibited by the C_3 to C_6 groups is similar, as well as the individual $C_mH_n^+$ profiles. The similarity of the mass spectra at these intensities suggests that the same dissociative states are reached although necessarily by different pathways at each pulse length. However, as the intensity increases under femtosecond irradiation, the individual profiles of the $C_2H_n^+$ to $C_5H_n^+$ groups alter. At the lower intensities fragmentation pathways favour a higher yield of $C_mH_3^+$ species ($m = 2$–5) in comparison to the naked C_m^+ fragment. For tetracene, at an intensity of $\sim$1.5–2.7 $\times$ 10^{15} W cm^{-2} fragmentation pathways preferentially shift to the lone C_m^+ ion. The same trend is observed for anthracene and pentacene although the critical intensity at which the C_m^+ ion yield surpasses the $C_mH_3^+$ ion yield decreases with increasing molecular size. This observation has been discussed in terms of a moderate contribution to the C_m^+ ion yield from coulomb explosions of multiply charged transient ions. However, further experiments under various conditions are required to elucidate the mechanism of ionisation/fragmentation for these molecules under intense laser irradiation. For instance, it is possible a multi-electron excitation ionisation-mechanism is involved and has

been described by Lezius et al. [43] in relation to polyatomic systems irradiated using 40 fs, 800 nm pulses.

It has been shown that the principle difference between the nanosecond and femtosecond post-ionisation of the PAHs in the present work is the formation of the di- and trications in large numbers. One of the proposed new areas of research for the fourth generation light sources being designed around the world is to investigate the fragmentation of di- and trication. The present work has demonstrated that the formation of these di- and trications can be efficiently carried out using femtosecond irradiation at 800 nm.

Finally, for both nanosecond and femtosecond irradiation, fragmentation favouring even carbon groups of $C_mH_n^+$ for $m \geq 12$ is evident. In addition fragmentation in which pairs of hydrogen atoms are expelled from the parent and doubly ionised parent is also energetically favoured.

Acknowledgements

References

[1] K. Codling, L.J. Frasinski, J. Phys. B 26 (1993) 783.
[2] R.J. Levis, M.J. DeWitt, J. Phys. Chem. A 103 (1999) 6493.
[3] D.M. Lubman, Laser and Mass Spectrometry, Oxford University Press, New York, 1990.
[4] C. Grun, R. Heinicke, C. Weickhardt, J. Grotemeyer, Int. J. Mass Spectrom. 185–187 (1999) 307.
[5] K.W.D. Ledingham, R.P. Singhal, Int. J. Mass Spectrom. Ion Process. 163 (1997) 149.
[6] R. Weinkhauf, P. Aicher, G. Wesley, J. Grotemeyer, E.W. Schlag, J. Phys. Chem. 98 (1994) 8381.
[7] K.W.D. Ledingham, C. Kosmidis, S. Georgiou, S. Couris, R.P. Singhal, Chem. Phys. Lett. 555 (1995) 247.
[8] X. Fang, K.W.D. Ledingham, P. Graham, D.J. Smith, T. McCanny, R.P. Singhal, A.J. Langley, P.F. Taday, Rapid. Commun. Mass Spectrom. 13 (1999) 1390.
[9] D.J. Smith, K.W.D. Ledingham, R.P. Singhal, H.S. Kilic, T. McCanny, A.J. Langley, P.F. Taday, C. Kosmidis, Rapid. Commun. Mass Spectrom. 12 (1998) 813.
[10] K.W.D. Ledingham, R.P. Singhal, D.J. Smith, T. McCanny, P. Graham, H.S. Kilic, W.X. Peng, S.L. Wang, A.J. Langley, P.F. Taday, C. Kosmidis, J. Phys. Chem. A 102 (1998) 3002.
[11] A.D. Tasker, L. Robson, K.W.D. Ledingham, T. McCanny, P. McKenna, C. Kosmidis, P. Tzallas, D.A. Jaroszynski, D.R. Jones, R.C. Issac, S. Jamison, J. Phys. Chem. A 106 (2002) 4005.
[12] A.N. Markevitch, N.P. Moore, R.J. Levis, Chem. Phys. 267 (2001) 131.
[13] I.S. Borthwick, PhD Thesis, University of Glasgow, 1993.
[14] S.M. Hankin, X. Fang, K.W.D. Ledingham, R.P. Singhal, T. McCanny, L. Robson, A.D. Tasker, C. Kosmidis, P. Tzallas, A.J. Langley, P.F. Taday, E. Divall, CLF RAL Annual Report RAL-TR-2000-034, 1990–2000, p. 89.
[15] C.J. McLean, P.T. McCombes, R. Jennings, K.W.D. Ledingham, R.P. Singhal, Nucl. Instrum. Meth. Phys. Res. B 62 (1991) 285.
[16] D.A. Jaroszynski, B. Ersfeld, G. Giraud, S. Jamison, D.R. Jones, R.C. Issac, B.M.W. McNeil, A.D.R. Phelps, G.R.M. Robb, H. Sandison, G. Vieux, S.M. Wiggins, K. Wynne, Nucl. Instrum. Meth. Phys. Res. 445 (2000) 317.
[17] E. De Hoffman, Mass Spectrometry Principles and Applications, Wiley, New York, 1996.
[18] D. Schröder, J. Loos, H. Schwarz, R. Thissen, D.V. Preda, L.T. Scott, D. Caraiman, M.V. Frach, D.K. Bohme, Helv. Chim. Acta 84 (2001) 1625.
[19] J. Posthumus (Ed.), Molecules and Clusters in Intense Laser Fields, Cambridge University Press, 2001.
[20] L. Robson, K.W.D. Ledingham, A.D. Tasker, P. McKenna, T. McCanny, C. Kosmidis, D.A. Jaroszynski, D.R. Jones, R.C. Issac, S. Jamison, Chem. Phys. Lett. 360 (2002) 382.
[21] A.M. Muller, C.J.G.J. Uiterwaal, B. Witzel, J. Wanner, K.-L. Kompa, J. Chem. Phys. 112 (2000) 9289.
[22] A. Assion, T. Baumert, M. Bergt, T. Brixner, B. Kiefer, V. Seyfried, M. Strehle, G. Gerber, Science 282 (1998) 919.
[23] P. Tzallas, C. Kosmidis, J.G. Philis, K.W.D. Ledingham, T. McCanny, R.P. Singhal, S.M. Hankin, P.F. Taday, A.J. Langley, Chem. Phys. Lett. 343 (2001) 91.
[24] K.W.D. Ledingham, D.J. Smith, R.P. Singhal, T. McCanny, P. Graham, H.S. Kilic, W.X. Peng, A.J. Langley, P.F. Taday, C. Kosmidis, J. Phys. Chem. A 103 (1999) 2952.
[25] S.C. O'Brien, J.R. Heath, R.F. Curl, R.E. Smalley, J. Chem. Phys. 88 (1988) 220.
[26] C. Cornaggia, P. Herring, Phys. Rev. A 62 (2000) 023403.
[27] L. Quaglia, C. Cornaggia, Phys. Rev. Lett. 84 (2000) 4565.
[28] B.S. Prall, M.J. DeWitt, R.J. Levis, J. Chem. Phys. 7 (1999) 2865.
[29] N. Nakashima, S. Shimizu, T. Yatsuhashi, S. Sakabe, Y.J. Izawa, Photochem. Photobiol. C: Photochem. Rev. 1 (2000) 131.
[30] M.J. DeWitt, R.J. Levis, J. Chem. Phys. 110 (1999) 11368.
[31] S.M. Hankin, D.M. Villeneuve, P.B. Corkum, D.M. Rayner, Phys. Rev. A 64 (2001) 013405.
[32] M.J. DeWitt, R.J. Levis, Phy. Rev. Lett. 81 (1998) 5101.
[33] L.V. Keyldish, Sov. Phys. JETP 20 (1965) 1307.
[34] M.J. DeWitt, R.J. Levis, J. Chem. Phys. 108 (1998) 7739.

[35] D.J. Smith, K.W.D. Ledingham, R.P. Singhal, T. McCanny, P. Graham, H.S. Kilic, P. Tzallas, C. Kosmidis, A.J. Langley, P.F. Taday, Rapid. Commun. Mass Spectrom. 13 (1999) 1366.

[36] C. Cornaggia, Phys. Rev. A 52 (1995) R4328.

[37] W. Dietz, H.J. Neusser, U. Boesl, E.W. Schlag, Chem. Phys. 66 (1982) 105.

[38] U. Bosel, H.H. Neusser, E.W. Schlag, J. Chem. Phys. 72 (1980) 4327.

[39] M. Castillejo, S. Couris, E. Koudoumas, M. Martin, Chem. Phys. Lett. 308 (1999) 373.

[40] D.J. Smith, K.W.D. Ledingham, H.S. Kilic, T. McCanny, W.X. Peng, R.P. Singhal, C. Kosmidis, A.J. Langley, P.F. Taday, J. Phys. Chem. 102 (1998) 2519.

[41] H. Sakai, H. Stablefeldt, E. Constant, M.Y. Ivanov, D.R. Matusek, J.S. Wright, P.B. Corkum, Phys. Rev. Lett. 81 (1998) 2217.

[42] K.P. Aicher, U. Wilhelm, J. Grotemeyer, J. Am. Soc. Mass. Spectrom. 6 (1995) 1059.

[43] M. Lezius, V. Blanchet, D.M. Rayner, D.M. Villeneuve, A. Stolow, M.Y. Ivanov, Phys. Rev. Lett. 86 (2001) 51.